HYDROLOGICAL PROCESSES
Hydrol. Process. **22**, 4789–4801 (2008)
Published online 25 July 2008 in Wiley InterScience
(www.interscience.wiley.com) DOI: 10.1002/hyp.7099

Observations and model estimates of diurnal water temperature dynamics in mosquito breeding sites in western Kenya

K. P. Paaijmans,[1,2]* A. F. G. Jacobs,[1] W. Takken,[2] B. G. Heusinkveld,[1] A. K. Githeko,[3] M. Dicke[2] and A. A. M. Holtslag[1]

[1] *Meteorology and Air Quality, Wageningen University, Wageningen, The Netherlands*
[2] *Laboratory of Entomology, Wageningen University, Wageningen, The Netherlands*
[3] *Kenya Medical Research Institute, Climate and Human Health Research Unit, Kisumu, Kenya*

Abstract:

Water temperature is an important determinant of the growth and development of malaria mosquito immatures. To gain a better understanding of the daily temperature dynamics of malaria mosquito breeding sites and of the relationships between meteorological variables and water temperature, three clear water pools (diameter × depth: 0·16 × 0·04, 0·32 × 0·16 and 0·96 × 0·32 m) were created in Kenya. Continuous water temperature measurements at various depths were combined with weather data collections from a meteorological station. The water pools were homothermic, but the top water layer differed by up to about 2 °C in temperature, depending on weather conditions. Although the daily mean temperature of all water pools was similar (27·4–28·1 °C), the average recorded difference between the daily minimum and maximum temperature was 14·4 °C in the smallest versus 7·1 °C in the largest water pool. Average water temperature corresponded well with various meteorological variables. The temperature of each water pool was continuously higher than the air temperature. A model was developed that predicts the diurnal water temperature dynamics accurately, based on the estimated energy budget components of these water pools. The air–water interface appeared the most important boundary for energy exchange processes and on average 82–89% of the total energy was gained and lost at this boundary. Besides energy loss to longwave radiation, loss due to evaporation was high; the average estimated daily evaporation ranged from 4·2 mm in the smallest to 3·7 mm in the largest water pool. Copyright © 2008 John Wiley & Sons, Ltd.

KEY WORDS Water temperature fluctuations; water energy budget; evaporation; aquatic insect ecology; malaria mosquito immatures; shallow water

Received 14 November 2007; Accepted 23 May 2008

INTRODUCTION

Climate plays a major role in distribution and abundance of insect species (Andrewartha and Birch, 1954; Sutherst *et al*., 1995). Being poikilothermic, insects are unable to internally regulate their body temperature and consequently their metabolic rate. Therefore, processes such as activity, growth and development depend on the temperature of the insect's direct environment. In general, within a certain temperature range, insects experience an increased growth rate at higher temperatures (Atkinson, 1994).

This temperature dependency applies to the immatures of mosquitoes that transmit malaria as well. With over one million deaths and between 350 and 500 million acute cases annually (WHO, 2005), malaria remains one of the most important and widespread tropical infectious diseases in the world. Over 75% of mortality cases relate to children living in sub-Saharan Africa (Breman, 2001), where the two sibling mosquito species *Anopheles arabiensis* Patton and *An. gambiae* Giles sensu stricto (hereafter referred to as *An. gambiae*), both belonging to the *An. gambiae* Giles sensu lato complex (hereafter referred to as *An. gambiae* s.l.), are important vectors of the pathogen.

The immature stages of these mosquitoes (an egg stage, four larval stages and a pupal stage) are aquatic and found in transient, sunlit and small water pools (Gillies and DeMeillon, 1968; Gillies and Coetzee, 1987; Gimnig *et al*., 2001), the availability of which depends on precipitation (Gimnig *et al*., 2001; Fillinger *et al*., 2004; Koenraadt *et al*., 2004). Typical examples of breeding sites are burrow pits, road puddles, tyre tracks and animal hoof prints and the reader is referred to the paper by Mutuku and colleagues (2006) for illustrations.

Being confined to their habitats, mosquito larvae are exposed to diurnal fluctuations in water temperature (Jepson *et al*., 1947; Huang *et al*., 2006). How these diurnal fluctuations in water temperature will affect insect development will depend on the magnitude and duration of the alternating phases (Huffaker, 1944). In general, higher temperatures will result in faster larval development, but in smaller females, as is observed in various mosquito species (Hagstrum and Workman, 1971; Shelton, 1973;

* Correspondence to: K. P. Paaijmans, Center for Infectious Disease Dynamics/Entomology Department, Pennsylvania State University, 19A Chemical Ecology Lab, University Park, PA 16802, USA.
E-mail: krijn@paaijmans.nl

Tun-Lin *et al.*, 2000). The development and growth of larvae of *An. gambiae* s.l. is also temperature-dependent (Lyimo *et al.*, 1992; Bayoh and Lindsay, 2003).

Water temperature is governed by various parameters, such as habitat geometry (Minakawa *et al.*, 2004), altitude, land cover type or canopy overgrowth (Munga *et al.*, 2006), water turbidity (Paaijmans *et al.*, 2008), presence of algae or aquatic vegetation, soil properties and local (micro)climate. The relationships between weather and the water temperatures of breeding sites of *An. gambiae* s.l. remain unknown, in spite of the fact that water temperature affects the growth, development and survival of the mosquito immatures, which affects the abundance, dynamics and fitness of the adult vector population and consequently the transmission rate of malaria. To understand and predict water temperature dynamics, fundamental knowledge of the various gains, losses and transfers of energy involved within water pools and at its boundaries are required; after all, fluctuations in water temperature are caused by the natural variation in energy fluxes in the atmospheric, water and soil layers.

Energy budgets of water pools have been studied but the majority focused on larger systems such as lakes (Keijman, 1974; Fraedrich *et al.*, 1977; Frempong, 1983), reservoirs (De Bruin, 1982), aquaculture ponds (Losordo and Piedrahita, 1991; Zhu *et al.*, 2000), rivers (Webb and Zhang, 1997; Evans *et al.*, 1998; Meier *et al.*, 2003) or ditches (Jacobs *et al.*, 1997), all being larger and deeper than typical breeding habitats of *An. gambiae* s.l.

Detailed knowledge of all energy budget components will enable one to predict water temperatures in an area using local weather data as input. Water temperatures were studied in great detail by monitoring them at various depths in three shallow and clear water pools of different size in western Kenya, in combination with weather data collections from a meteorological station. The objectives were (i) to study the diurnal water temperature dynamics in the water pools, (ii) to examine the effects of meteorological conditions on these dynamics and (iii) to develop and evaluate a model that predicts the diurnal water temperature behaviour by estimating all terms of the heat budget with local weather data.

MATERIAL AND METHODS

All measurements were carried out at the Kenya Medical Research Institute (KEMRI), near Kisumu, Kenya between 16 March (Day Of Year 75) and 5 May 2005 (DOY 125), a period that experienced frequent rains. The local soil was black cotton soil, which consists of 12% sand, 28% silt and 60% clay in the top 0·20 m and 24% sand, 16% silt and 60% clay at a depth of 0·2–1·2 m (Muchena, 1976). Both experimental areas were covered with grass, which was kept short.

Meteorological station (0°04′36·390″S; 34°40′34·770″E; 1126 m above sea-level)

Wind speed at 2 and 10 m height (cup anemometers; Meteorology and Air Quality, Wageningen University), incoming shortwave and longwave radiation at 1·5 m above ground (CM11 and CG1, respectively; Kipp & Zonen, The Netherlands), temperature and relative humidity at 2 m above ground (ventilated probe; Vaisala, Finland) and precipitation (rain gauge; Eijkelkamp, The Netherlands) were measured.

Water station

Nearby this meteorological station different-sized circular water pools were created by digging holes in the ground: a small-sized water pool (hereafter referred to as SP: diameter 0·16 m, water depth 0·04 m, volume 0·8 L), a medium-sized water pool (MP: diameter 0·32 m, water depth 0·16 m, volume 12·9 L) and a large-sized water pool (LP: diameter 0·96 m, water depth 0·32 m, volume 231·6 L). The holes were lined with semi-transparent plastic (0·13 mm thick), pressed tightly against the soil to maximize plastic–soil contact and filled with clear tap water that originated from a well at KEMRI, up to 10 mm under the brim. The plastic was kept in place by a metal ring (diameter 50 mm larger than the water pool). A uniform water level was maintained by adding or removing water to the starting level every morning to compensate for evaporation or precipitation, respectively. The setup was cleaned and refilled on a weekly basis.

Water temperatures were measured in the centre of the water pools at various depths (SP: 1 and 30 mm; MP: 1, 30, 60 and 120 mm; LP: 1, 30, 60, 120 and 240 mm below the air–water interface) with glass bead thermistors (NTC BEAD 4K7, Thermometrics, USA). These thermistors were placed in stainless steel tubes (1·8 mm diameter) which were filled with heat conductivity paste and attached waterproof to the wiring with white heat-shrink material. The floating equipment (LP, Figure 1) was made of Teflon tubes (diameter 6 mm), Teflon rings (diameter 19 mm) and polystyrene balls (diameter 40 mm), all connected with Perspex tubes (diameter 4 mm). Soil temperatures were measured with similar thermistors at 0·05, 0·17 and 0·33 m depth in the undisturbed soil in the middle of the experimental area.

Data analysis

All data were totalled (precipitation) or averaged (remaining variables) at 5-min intervals (meteorological station) or 15-min intervals (water station) and stored in a 21x Microdatalogger (Campbell Scientific Inc., UK). Owing to a few days with missing data and the cleaning of the setup on a weekly basis, 40 days are used for analysis. The times mentioned in this paper are local times (UTC + 3).

Nine days were chosen for a detailed energy budget study: three consecutive days with predominantly clear skies (DOY 86–88), three consecutive days with

DOI: 10.1002/hyp

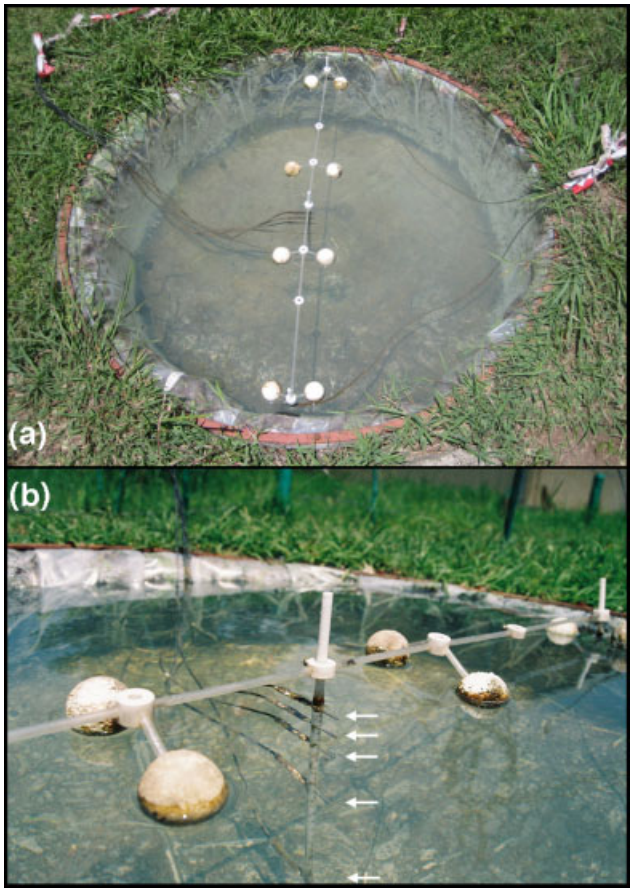

Figure 1. (a) Experimental setup: measuring water temperatures at various depths in a large-sized water pool (b) Close-up of the floating equipment. The arrows indicate the thermistors at various depths in the water column

overcast conditions (DOY 95–97) and three consecutive days with heavier overcast and heavy precipitation (DOY 117–119). Table I shows some meteorological variables for the days that were selected for this study.

Correlations between the measured water temperatures and various meteorological variables were analysed using SPSS software (version 12·0·1, SPSS Inc., Chicago, IL). The statistical significance of the correlations and Spearman's correlation coefficient (ρ) are given. This coefficient indicates the magnitude of the association between two variables.

Energy budgets

It appeared that the water temperatures measured at the various depths were similar throughout each diurnal cycle, making it possible to treat each water pool as a homogeneous system.

Radiative heat exchange at a water pool

The total absorbed radiation in a water pool, R_a (W m^{-2}), is calculated by:

$$R_a = R_s^* + \varepsilon_w(R_l^{\downarrow} - \sigma {T_w}^4) \quad (1)$$

where R_s^* (W m^{-2}) is the available net shortwave radiation, ε_w (0·97) the emissivity value for water (Losordo and Piedrahita, 1991), $R_l^{\downarrow}$ (W m^{-2}) the incoming longwave atmospheric radiation, σ ($5{\cdot}67 \times 10^{-8}$ W m^{-2} K^{-4}) the Stefan–Boltzmann constant and T_w (K) the temperature of the water pool. R_s^* is parameterized as follows (Figure 2a):

$$R_s^* = (1 - a_w)[\beta + (1 - \beta)(1 - a_s)]R_s^{\downarrow} \quad (2)$$

where a_w (0·06) is the albedo of the water pool (Budyko, 1956), β the proportion of total incoming solar radiation at the water surface that is absorbed in the upper water layer, which is approximately 0·4–0·5 (Losordo and Piedrahita, 1991); in this study a value of 0·45 was used for β since all the near-infrared radiation (constituting approximately 45% of all incoming shortwave radiation) is absorbed in the upper layer of each water pool. In addition, a_s (0·20) is the albedo of the soil at the water–soil interface (Arya, 2001) and $R_s^{\downarrow}$ (W m^{-2}) is the incoming shortwave radiation. Because the plastic that was used in this study was not completely transparent, it will reflect part of the incoming solar radiation at the bottom. To compensate for this effect, the albedo of the soil was increased by 0·1.

Table I. Total daily incoming shortwave and longwave radiation load, daily average air temperature, daily average water temperatures of the three different sized water pools and daily rainfall quantity measured during a period with clear days, a period with overcast days and a period that experienced heavy overcast and heavy precipitation

DOY	Clear days			Overcast days			Extremely overcast days		
	86	87	88	95	96	97	117	118	119
$R_s^{\downarrow}$ (MJ m^{-2})	26·3	26·2	26·8	20·4	20·3	18·5	21·8	07·9	10·5
$R_l^{\downarrow}$ (MJ m^{-2})	33·3	32·6	32·2	33·9	34·7	34·0	34·8	35·5	34·8
T_a (°C)	23·9	23·0	23·8	23·1	21·7	22·4	25·0	21·4	21·4
r_a (mm)	05·8	02·0	00·2	00·0	08·8	04·6	05·4	40·6	03·4
$T_{w,s}$ (°C)	27·9	28·0	28·3	26·7	26·4	26·4	28·7	24·6	25·0
$T_{w,m}$ (°C)	28·5	28·6	28·6	27·0	26·8	26·7	29·0	25·2	25·3
$T_{w,l}$ (°C)	28·8	29·1	28·9	27·5	27·1	27·0	29·1	25·9	25·3

$R_s^{\downarrow}$ incoming shortwave radiation flux density, $R_l^{\downarrow}$ incoming longwave radiation flux density, T_a air temperature at two meters, r_a rainfall quantity, $T_{w,s}$ water temperature of the SP, $T_{w,m}$ water temperature of the MP, $T_{w,l}$ water temperature of the LP.

DOI: 10.1002/hyp

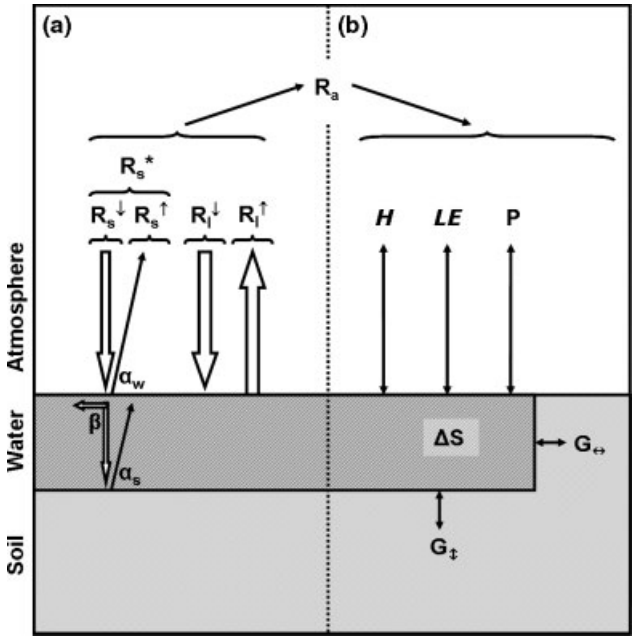

Figure 2. Conceptual model of radiation and energy fluxes at the air–water and soil–water interfaces of small, shallow and clear water pools: (a) radiative heat exchange; and (b) non-radiative heat exchange. R_a total absorbed radiation in a water pool, $R_s{}^*$ available net shortwave radiation, $R_s{}^\downarrow$ incoming shortwave radiation, $R_s{}^\uparrow$ outgoing shortwave radiation, $R_l{}^\downarrow$ incoming longwave radiation, $R_l{}^\uparrow$ outgoing longwave radiation, a_w the albedo of the water pool, β the proportion of total incoming solar radiation at the water surface that is absorbed in the upper water layer, a_s the albedo of the soil at water-soil interface, H sensible heat flux density and LE latent heat flux density, P amount of energy stored in or extracted from a water pool due to precipitation, $G_\updownarrow$ soil heat flux density vertically, $G_\leftrightarrow$ soil heat flux density sideways, ΔS energy storage

Non-radiative heat exchange at a water pool

The total absorbed radiation by a water pool is partitioned (Figure 2b) as follows:

$$R_a = H + LE + P + G + \Delta S \tag{3}$$

where H (W m^{-2}) is the sensible heat flux, LE (W m^{-2}) the evaporation or latent heat flux, P (W m^{-2}) the amount of energy stored in or extracted from a water pool due to precipitation, and G (W m^{-2}) the heat flux between water and soil. ΔS (W m^{-2}) is the amount of remaining energy that is stored in or extracted from the water and determines the magnitude of the change in water temperature.

The movement of heat energy from the water surface to the atmosphere by conduction and convection, the sensible heat flux H, is parameterized as (Arya, 2001):

$$H = \rho_a c_p C_h u(T_w - T_a) \tag{4}$$

where ρ_a (kg m^{-3}) is the density of air, c_p (J kg^{-1} K^{-1}) the specific heat capacity of air at constant pressure, C_h the sensible heat transfer coefficient at 2 m height, u (m s^{-1}) the wind speed at 2 m, T_a (K) the air temperature at 2 m.

The movement of heat energy from the water surface to the atmosphere due to evaporation of water, the latent heat flux LE, is parameterized as (Arya, 2001):

$$LE = \rho_a L C_w u(q_s - q_a) \tag{5}$$

where L (J kg^{-1}) is the latent heat of evaporation, C_w the water vapour transfer coefficient at 2 m height, q_s (kg kg^{-1}) and q_a (kg kg^{-1}) the saturation-specific humidity and specific humidity at 2 m height, respectively. The latent heat of evaporation is temperature dependent and calculated according to Fritschen and Gay (1979). The saturation specific humidity for water vapour and air are estimated using the Clausius–Clapeyron equation.

Owing to the similarity of the transfer mechanisms of heat and water vapour (Reynolds analogy), one may assume that $C_h \approx C_w$. Both transfer coefficients were initially approximated over the surrounding grassland with the Monin–Obukhov Similarity Theory (Arya, 2001) using a roughness length for momentum (z_{0M}) of 1 mm above short grass (Campbell and Norman, 2000) and a roughness length for heat (z_{0H}) of $z_{0H} = z_{0M}/10$ (Beljaars and Holtslag, 1991), giving $C_h = 0{\cdot}003$.

Although there was a difference between the temperature of the water pools and the temperature of the rain droplets, and precipitation clearly affected the water temperature, it appeared from the calculations that the energy transferred advectively by precipitation, P, could be ignored in our model.

The movement of heat energy by conduction through the soil, the soil heat flux G, is described by the slightly modified Fourier's Law. The energy exchange between soil and water is calculated in both a vertical and sideways direction and is parameterized as:

$$G = -\lambda_s \frac{\delta T}{fD} \tag{6}$$

where λ_s (W m^{-1} K^{-1}) is the thermal conductivity of the soil, which is 1·2 for the saturated soil (Campbell and Norman, 2000). It was assumed that soil temperatures were similar and behaved homogeneously over a horizontal plane.

Regarding the vertical soil heat flux, δT (K) was the temperature difference between the temperature of the water pool and the soil temperature at depth d (m), the depth of the water pool. Regarding the horizontal soil heat flux, δT was the temperature difference between water temperature and average soil temperature over depth d. The damping depth D (m) of the diurnal temperature wave in the soil was multiplied by f (0·3), a factor that depends on d and had to be applied at the SP only, since the surrounding soil will influence the temperature of the small water volume, whereas this water volume will have relatively less impact on the temperature of the surrounding soil. This factor was determined by trial and error. D is parameterized as (Monteith and Unsworth, 1990):

$$D = \frac{z_1 - z_2}{\ln(A_{z2}) - \ln(A_{z1})} \tag{7}$$

where z (m) is the measurement depth in the soil and A_z the amplitude of the soil temperature at depth z.

Finally the water temperature is given by:

$$T_{w,n} = T_{w,n-1} + \frac{\Delta S \Delta t}{\rho_w c_w d} \tag{8}$$

DOI: 10.1002/hyp

where n (s) is the time step. An initial value needs to be given to $T_{w,0}$, which was done by using the observed initial water temperature.

RESULTS

Meteorological variables

The average daily incoming radiation load over the study period was 21·9 (±0·6 standard error of the mean; range 7·9–27·1) MJ m^{-2} day^{-1} for shortwave and 33·7 (±0·1; range 30·6–35·6) MJ m^{-2} day^{-1} for longwave radiation. The average daily air temperature was 23·4 (±0·2; range 21·4–25·5) °C, with an average daily minimum temperature of 18·5 (±0·1; range 14·7–21·2)°C and an average daily maximum temperature of 29·4 (±0·2; range 24·4–32·9) °C. A total of 32 days experienced precipitation ranging from 0·2 (lower rain-gauge threshold level) to 40·6 mm day^{-1}, the total precipitation being 270·3 mm in this period and the highest recorded intensity 9·5 mm in 5 min.

Observations of diurnal water temperature dynamics

Apart from the upper water layer, the water temperatures measured in the deeper layers were similar and behaved homogeneously throughout each diurnal temperature cycle. The top water layer (thickness 2 mm) differed in temperature and in its diurnal temperature dynamics (Figure 3) compared with the deeper layers. In general, the upper water layer of the SP and MP was cooler (up to approximately 2 °C) during most of the afternoon and during night-time, but became warmer (up to about 1 °C) during the first hours after sunrise. This difference in water temperature was larger on clear days compared with overcast days. The difference in temperature between the top water layer and the layers beneath in the LP showed similar dynamics, whereby the top layer remained cooler during larger parts of the day or during the whole day compared with the smaller water pools.

Rainfall clearly affected the difference between the temperature of the top water layer and the layers beneath, but the magnitude of this difference and whether it results in an increase or decrease in difference will depend on parameters such as habitat dimensions, the existing water temperature, the temperature of rainwater, the duration and amount of precipitation and the time of day.

The SP reached its daily minimum (night-time) and maximum (day-time) temperature earlier than the MP and LP did (Figures 4–6). The times at which these minimum and maximum values were recorded differed at various weather conditions. On a spatial scale, the SP showed the largest diurnal temperature fluctuations and this water pool heated (day-time) and cooled (night-time) more than the larger water pools (Figures 4–6). The daily average minimum water temperature recorded during the study period was 22·4 (±0·1; range 20·8–23·9)°C in the SP, 23·9 (±0·1; range 22·3–25·2)°C in the MP and 25·1 (±0·1; range 23·1–26·2)°C in the LP. The daily average maximum water temperature was 36·8 (±0·3; range 29·4–39·0)°C in SP, 33·9 (±0·3; range 27·8–35·8)°C in MP and 32·1 (±0·2; range 27·5–33·8)°C in LP. This resulted in average differences between daily minimum and maximum water temperature of 14·4 (±0·3 range 7·8–16·8) °C, 10·1 (±0·3 range 4·7–12·2)°C and 7·1 (±0·2 range 3·8–8·5)°C in the SP, MP and LP, respectively.

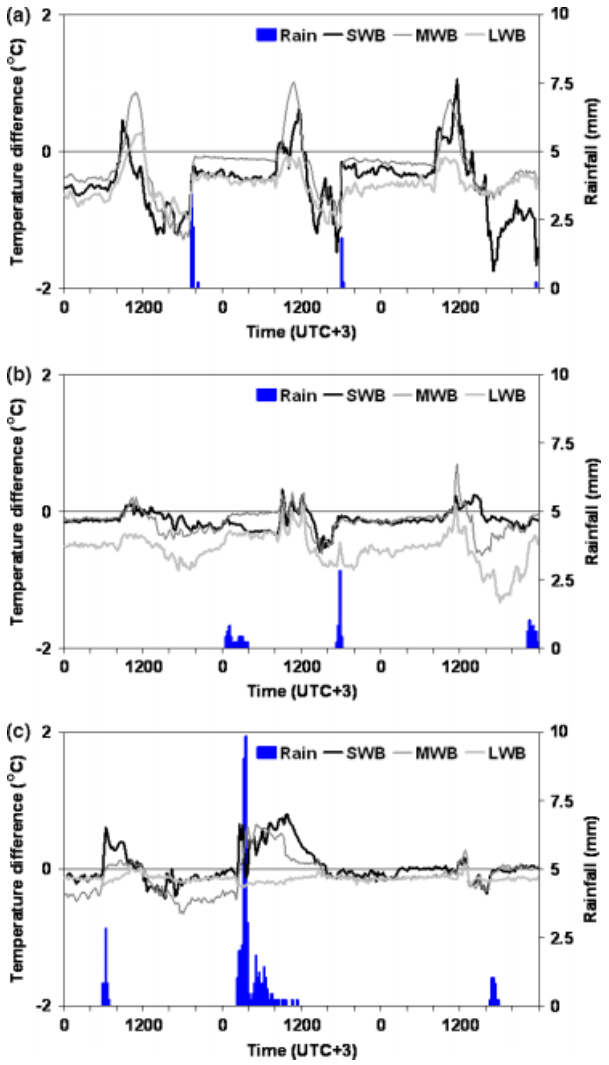

Figure 3. Temperature difference between top water layer (thickness of 2 mm) and the deeper water layer(s) in the SP (black line), the MP (dark grey line) and the LP (light grey line) and rainfall (vertical bars) on (a) DOY 86–88, (b) DOY 95–97, and c) DOY 117–119. Values above 0 °C indicate a warmer top layer

The daily minimum water temperature significantly ($\chi^2 = 87{\cdot}2$; $P < 0{\cdot}001$) increased when habitat size increased, whereas the daily maximum water temperature and the daily difference between minimum and maximum water temperature significantly ($\chi^2 = 76{\cdot}3$ and $\chi^2 = 90{\cdot}5$, respectively; $P < 0{\cdot}001$) decreased when habitat size increased. Besides the difference in temperature between the water pools, the temperature increase and decrease per unit time during daytime was higher in smaller water pools.

Despite these differences on a temporal and spatial scale, the average daily water temperature in the different water pools was similar: 27·4 (±0·2; range 24·6–29·1)°C

DOI: 10.1002/hyp

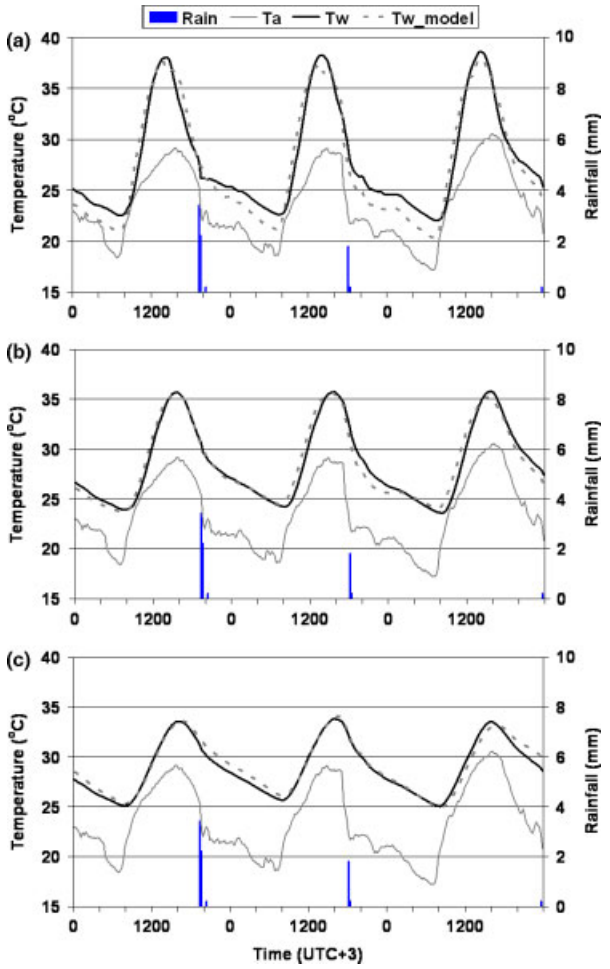

Figure 4. Measured air temperature (T_a) and measured precipitation and the measured (T_w: average water temperature of all water layers, except for the top water layer) and modelled (T_{w_model}) diurnal temperature behaviour of (a) the small-sized water pool, (b) the medium-sized water pool, and (c) the large-sized water pool, during DOY 86–88

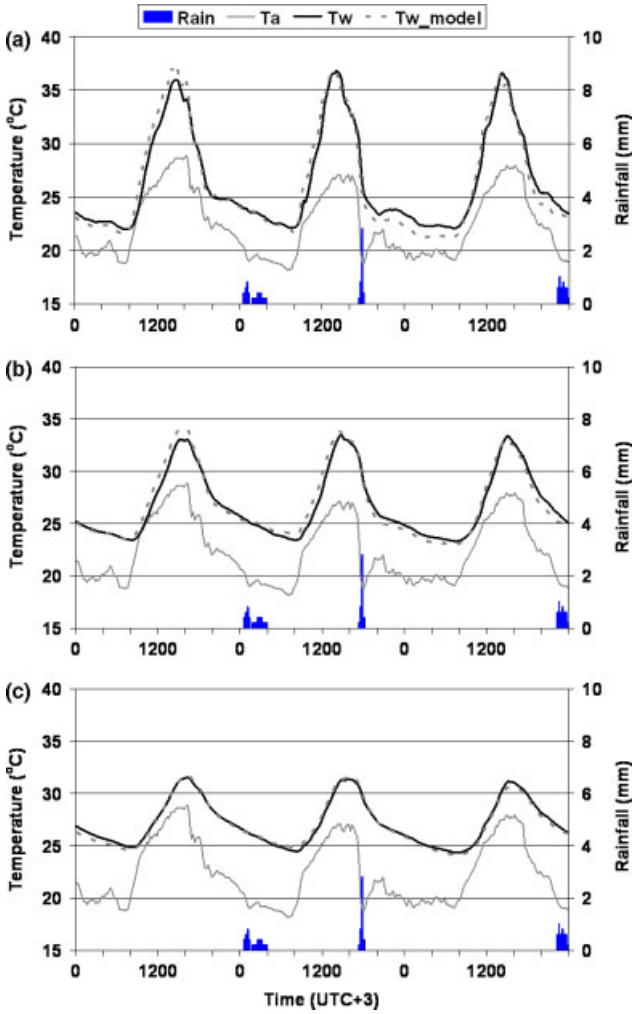

Figure 5. Measured air temperature (T_a) and measured precipitation and the measured (T_w: average water temperature of all water layers, except for the top water layer) and modelled (T_{w_model}) diurnal temperature behaviour of (a) the small-sized water pool, (b) the medium-sized water pool, and (c) the large-sized water pool, during DOY 95–97

in the SP, 27·8 (±0·2; range 25·2–29·0)°C in the MP and 28·1 (±0·2; range 25·3–29·3)°C in the LP.

The water temperatures in all our water pools were higher than the air temperature at 2 m above ground every day at any given time (Figures 4–6), which has important consequences for the behaviour of the sensible and latent heat fluxes, as will be shown later. The average differences between daily minimum air and daily minimum water temperatures during the study period were 3·9 (±0·1; range 2·2–5·2), 5·3 (±0·1; range 3·7–6·8) and 6·5 (±0·1; range 4·4–8·1) at the SP, MP and LP, respectively. The average differences between the daily maximum air and daily maximum water temperatures were 7·6 (±0·2; range 4·8–10·2), 4·7 (±0·2; range 2·2–7·5) and 2·9 (±0·2; range 0·3–5·6) at the SP, MP and LP, respectively.

Relations between water temperatures and meteorological variables

In general, the small-sized water pool reacted more dynamically to sudden changing meteorological variables. Its temperature corresponded better to incoming solar radiation. This effect was most distinct on clear days where a change in incoming solar radiation load ($\Delta R_s^{\downarrow}$) and a change in water temperature (ΔT_w) were highly and significantly (15-min intervals; $P < 0{\cdot}001$) correlated (DOY 86–88; SP $\rho = 0{\cdot}78$, MP $\rho = 0{\cdot}57$, LP $\rho = 0{\cdot}49$).

During precipitation the water temperature increased or decreased, depending on various parameters as mentioned earlier. A decrease in water temperature was recorded during 75% (SP), 94·5% (MP) and 96·5% (LP) of the 15-min periods that experienced rainfall, with an average decrease of 0·45 (±0·1) in the SP, 0·25 (±0·0) in the MP and 0·17 (±0·0)°C in the LP. The maximum recorded decrease in water temperature during rainfall was 5, 2·6 and 1·4 °C in 15 min in the SP, MP and LP, respectively, on DOY 124 (17h45) when the highest rainfall intensity was recorded (19·3 mm in 15 min). There was a significant ($P < 0{\cdot}001$) but moderate correlation between the decrease in water temperature and the amount of rainfall (SP $\rho = -0{\cdot}59$; MP $\rho = -0{\cdot}54$; LP $\rho = -0{\cdot}57$).

The average increase in water temperature during rainfall was 0·11 (±0·02), 0·07 (±0·02) and 0·04 (±0·01)°C in the SP, MP and LP, respectively. The maximum

DOI: 10.1002/hyp

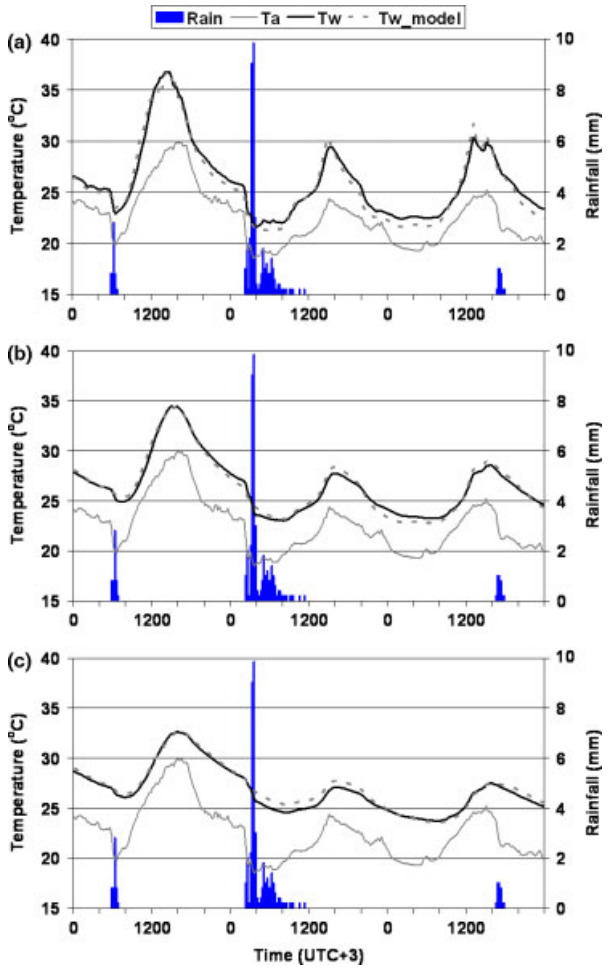

Figure 6. Measured air temperature (T_a) and measured precipitation and the measured (T_w: average water temperature of all water layers, except for the top water layer) and modelled (T_{w_model}) diurnal temperature behaviour of (a) the small-sized water pool, (b) the medium-sized water pool, and (c) the large-sized water pool, during DOY 117–119

recorded increase in water temperature during rainfall was 0·6, 0·2 and 0·1 °C in the SP, MP and LP, respectively.

The daily average water temperature corresponded highly and significantly with various meteorological variables (Table II), especially with the average air temperature at 0·1 and 2 m height. Such simple linear relationships make these meteorological variables good predictors of the daily average water temperature in water pools. The relations between water temperatures (average, minimum and maximum) and both average air temperature and total daily incoming solar radiation load are shown in Figures 7 and 8, respectively.

The daily maximum water temperature was highly and significantly ($P < 0{\cdot}001$) correlated with the daily total incoming solar radiation load and this correlation was best for the larger water pools (Figure 8; SP $\rho =$ 0·67; MP $\rho = 0{\cdot}86$; LP $\rho = 0{\cdot}90$). The daily minimum water temperature corresponded highly and significantly ($P < 0{\cdot}001$) with the daily average water temperature (SP $\rho = 0{\cdot}61$; MP $\rho = 0{\cdot}74$; LP $\rho = 0{\cdot}81$) and corresponded less well with the measured meteorological variables.

Table II. Correlations (Spearman's rho > 0·75 for at least one water pool) between the daily average water temperature and the daily average or daily total of various meteorological variables. All correlations were significant ($P < 0{\cdot}001$)

Average T_w vs.	SP ($n = 39$)	MP ($n = 40$)	LP ($n = 40$)
Average T_{10}	0·94	0·93	0·90
Average T_a	0·93	0·91	0·86
Average T_{-5}	0·89	0·89	0·86
Average max T_a	0·85	0·80	0·73
Average T_{-17}	0·80	0·84	0·82
Total $R_s{\downarrow}$	0·74	0·76	0·79

SP Small water pool; MP Medium water pool; LP Large water pool, T_w water temperature, T_{10} air temperature 10 cm above grass, T_a air temperature at 2 m above ground, T_{-5} soil temperature at 5 cm depth, max maximum, T_{-17} soil temperature at 17 cm depth, $R_s{\downarrow}$ incoming shortwave radiation load.

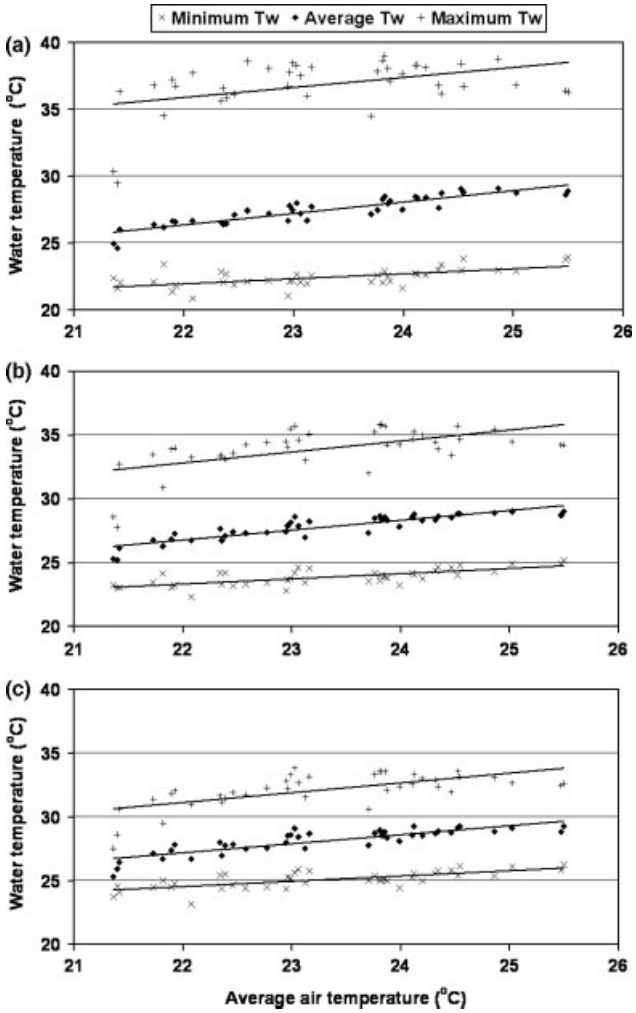

Figure 7. Minimum, average and maximum daily water temperatures (T_w) of (a) the small-sized water pool, (b) the medium-sized water pool, and (c) the large-sized water pool, plotted against the average daily air temperature. The black lines represent regression lines

Model estimates of diurnal water temperature variations

Model simulations for the three selected periods were executed and the results are shown in Figures 4–6. Generally, it can be observed that the modelled water temperature dynamics were similar to the measured

DOI: 10.1002/hyp

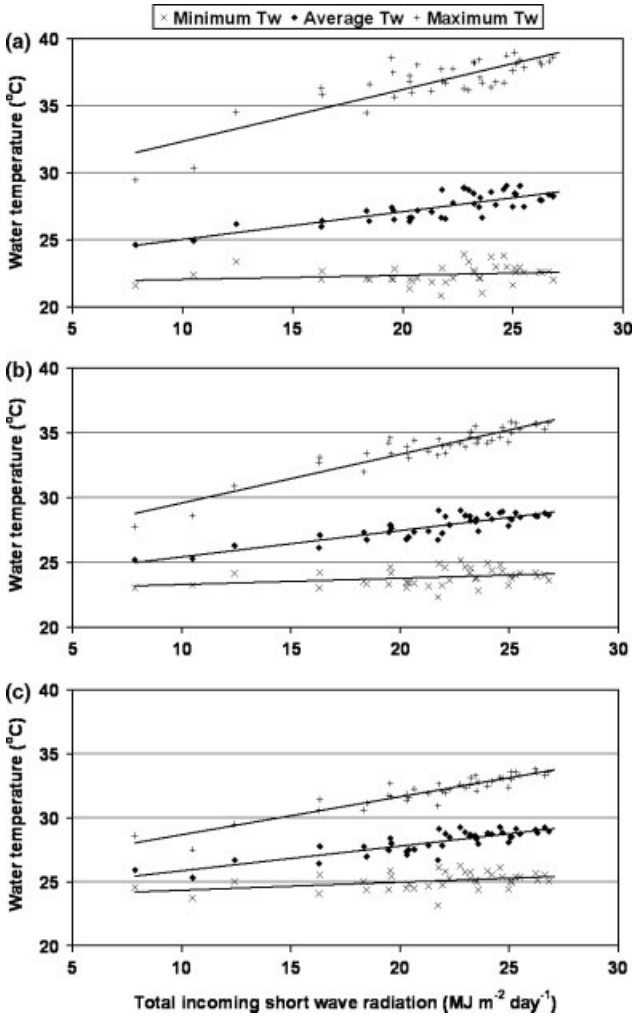

Figure 8. Minimum, average and maximum daily water temperatures (T_w) of (a) the small-sized water pool, (b) the medium-sized water pool, and (c) the large-sized water pool, plotted against the daily total incoming shortwave radiation. The black lines represent regression lines

water temperatures. Quantitatively, the maximum values, minimum values and changes of temperature during rainfall occurred more or less at the same time and were of the same magnitude.

A small dissimilarity between the modelled and measured water temperatures was obtained during nocturnal cooling of the SP, mainly during periods with clear days, whereby the modelled temperature was up to 2·0 °C lower than the actual water temperature. The largest dissimilarities (up to 2·5 °C in the SP) were obtained during the first hours after sunrise up to around local noon. This is due to the rapid increase in water temperatures whereby the modelled temperatures increased slightly earlier in time. However, as mentioned before, the diurnal course was similar and similar minimum and maximum temperatures were reached during the day and, therefore, the dissimilarities can be neglected.

Model estimates of the energy budget components

Table III shows the estimated energy gains and losses through the various terms of the energy budget during the second day of each selected period. The percentages given hereafter are averages over the entire study period.

Table III. Measured or modelled daily percentages of energy gains and losses at the water pools studied on the second day of each selected period where DOY 87 was clear, DOY 96 was overcast and DOY 118 was heavily overcast and rainy

	DOY 87			DOY 96			DOY 118		
	SP	MP	LP	SP	MP	LP	SP	MP	LP
Gains									
R_s^* (%)	34·5	32·8	32·9	28·5	27·1	26·6	13·7	13·7	14·0
$R_l^{\downarrow}$ (%)	52·4	49·8	50·0	59·6	56·7	55·6	75·9	75·9	77·2
$G_{\updownarrow}$ (%)	5·8	4·7	0·1	4·9	3·9	2·1	5·3	2·1	1·6
$G_{\leftrightarrow}$ (%)	2·5	0·9	0·2	2·2	1·1	0·7	1·6	0·5	0·1
ΔS (%)	4·8	11·8	16·9	4·9	11·2	15·1	3·4	7·7	7·2
Losses									
$R_l^{\uparrow}$ (%)	63·9	60·5	60·0	66·9	63·5	62·1	80·1	74·5	69·4
H (%)	2·9	3·0	3·0	3·1	3·2	3·1	1·8	2·3	2·8
LE (%)	19·6	18·7	18·5	17·8	17·0	16·2	9·1	10·4	11·6
$G_{\updownarrow}$ (%)	4·8	2·5	0·1	4·0	2·3	1·1	2·2	0·3	0·0
$G_{\leftrightarrow}$ (%)	3·7	2·5	0·0	2·7	1·9	1·4	2·3	0·5	0·8
ΔS (%)	5·0	12·8	18·4	5·4	12·1	16·1	4·5	12·1	15·4

R_s^* available net shortwave radiation, $R_l^{\downarrow}$ incoming longwave radiation, $R_l^{\uparrow}$ outgoing longwave radiation, $G_{\updownarrow}$ soil heat flux density vertically, $G_{\leftrightarrow}$ soil heat flux density sideways, ΔS energy storage, H sensible heat flux density and LE latent heat flux density.

Energy gained at the air–water interface through radiative processes contributed most to the total energy gained at the water pools: on average 88·1 (±0·2; range 85·1–91·6)%, 84·3 (±0·2; range 81·6–89·7)% and 82·9 (±0·3; range 79·3–91·1)% was gained by shortwave and longwave radiation at the SP, MP and LP, respectively. The relative importance of energy that was stored in the water increased with increasing water pool volume (the average percentage was 5·0 (±0·1; range 3·4–5·6) at the SP, 11·9 (±0·2; range 7·7–13·4) at the MP and 15·3 (±0·3; range 7·2–17·3) at the LP), whereas the contribution of the soil heat flux to energy gain (both vertical and sideways) decreased with increasing water pool volume, with the average percentage of the total soil heat flux being 6·9 (±0·2; range 3·5–9·4) at the SP, 3·8 (±0·2; range 1·8–5·6) at the MP and 1·8 (±0·1; range 0·3–3·8) at the LP.

Similar to the energy gains, the largest percentage of energy loss occurred at the air–water boundary: 88·6 (±0·3; range 85·8–92·2)%, 83·5 (±0·3; range 80·6–89·2)% and 81·8 (±0·4; range 77·7–89·6)% was lost at the SP, MP and LP, respectively, through longwave radiation, latent heat and sensible heat. The contribution of longwave radiation to the energy loss was largest: on average this percentage was 68·6 (±0·6; range 63·9–80·5)% at the SP, 65·9 (±0·5; range 60·5–79·2)% at the MP and 65·2 (±0·6; range 60·0–79·8)% at the LP.

Because the air temperature was lower than the water temperatures at all water pools at any given time of the day, there was a continuous heating of air above water pools (positive sensible heat flux). Since the water surface temperature is a direct measure of the saturated specific humidity at the water surface, assuming the

DOI: 10.1002/hyp

air near the water surface will be saturated, there was a continuous evaporation of water (positive latent heat flux). The percentage of energy loss through sensible heat was relatively small (an average contribution of 2–2·4% to the total loss at all water pools with a maximum of 3·2%), whereas the latent heat flux accounted for a large part of the energy lost; on average 17·6 (±0·6; range 8·6–23·4)% at the SP; 15·5 (±0·4; range 8·3–19·7)% at the MP and 14·7 (±0·4; range 8·2–18·5)% at the LP. The contribution of evaporation to the total energy loss decreased during the (heavy) overcast days.

Similar to the energy gains, the percentage of energy lost to the soil decreased with increasing water pool dimensions (6·4 (±0·3%; range 3·0–8·8)% at the SP, 4·5 (±0·2%; range 0·8–6·8)% at the MP and 2·8 (±0·2%; range 0·1–5·5)% at the LP), whereas the energy that was extracted from the water was more important for the larger water pools (5·0 (±0·1; range 3·9–6·1)% at the SP, 12·0 (±0·2; range 7·6–13·4)% at the MP and 15·4 (±0·2; range 9·7–18·4)% at the LP).

With respect to the terms that contributed to the gains as well as the losses of energy over the study period, it seemed that the gains and losses through the storage term (overall all water pools lost 0·1%) and through the soil heat (the SP gained on average 0·5%, the MP lost 0·6% and the LP lost 0·9%) were approximately of similar quantity. Contrarily, more longwave radiation was emitted from than received at the air–water interface of the water pools, resulting in an average loss of 10·4% at all water pools through this heat flux.

Taking a closer look at the evaporation rates, the small-sized water pool showed a higher evaporation (mm day^{-1}) during daytime than the large-sized water pool, but this situation was reversed during the night. During the study period, the average daily estimated evaporation was 4·2 (±0·2; range 1·6–5·9) mm at the SP, 3·8 (±0·1; range 1·6–5·0) mm at the MP and 3·7 (±0·1; range 1·6–5·1) mm at the LP.

DISCUSSION

The upper millimetres of a water pool are important in the larval population dynamics of *An. gambiae* s.l., as malaria mosquito larvae generally live horizontally near the air–water interface of aquatic habitats (Tuno *et al*., 2004). In this study it was demonstrated that the top layer (upper 2 mm) of each water pool differed in temperature from the layers underneath. During the afternoon and at night, the temperature of the top layer was up to 2 °C lower than the layers below, and during the first hours after sunrise, the temperature of this layer was up to about 1 °C higher, depending on weather conditions. The observed higher temperature of the top water layer during the first hours after sunrise is caused by the incoming radiation load combined with a relatively small difference between water and air temperature. Around local noon, the difference between air and water temperature becomes larger and more energy will be extracted from the top water layer due to evaporation (latent heat flux) and the heating of the air above the water surface (sensible heat flux), resulting in a lower temperature of the top water layer.

No stratification was observed in the small and clear water pools, meaning that the water in the pools was mixed well. The diurnal water temperature behaviour of the three different-sized water pools differed on both a spatial and a temporal scale. The small-sized water pool reached its minimum and maximum temperature at an earlier stage of the day than the larger ones. Spatially, higher daily maximum and lower daily minimum water temperatures were recorded when habitat dimension decreased. Water temperatures below 18 °C were not recorded (20·8 °C was the lowest recorded temperature in the SP). When larvae were reared at 18 °C in the laboratory, no adults emerged (Bayoh and Lindsay, 2003, 2004).

The same laboratory studies showed that no adults were emerging when larvae were reared above 32 °C. The larvae were, however, continuously exposed to constant temperatures. Apparently, as this study showed that 32 °C was regularly exceeded on both clear and overcast days in the water pools, larvae are able to withstand these higher temperatures, which are reached for a relatively short period during the day. The maximum temperature that larvae of *An. gambiae* s.l. can endure for a short period is believed to be 41 °C (Haddow, 1943; Jepson *et al*., 1947). Higher temperatures were lethal, but such extreme water temperatures were not recorded during this study; the average maximum water temperature was 36·8 (±0·3)°C in the smallest water pool. This temperature is near the temperature at which mosquito larvae have the highest development rate (Depinay *et al*., 2004).

These data show that mosquito immatures can be exposed to a wide temperature range under natural conditions, as the average recorded difference between the daily minimum and maximum water temperature was 14·4 °C in the SP with a maximum recorded difference of 16·8 °C. Therefore, they may experience many of the constant temperatures at which they are reared in laboratory experiments in one single diurnal temperature cycle.

Notwithstanding the spatial and temporal differences between water pools of different size, the average daily water temperature over the whole period was quite similar (27–28 °C) for all water pools. Similar mean water temperatures were found in The Gambia by Bayoh (2001) in puddles (27·1 °C) and in habitats in rice fields (27·4 °C). Laboratory studies revealed that 27 °C was the optimal temperature for the survival of *An. gambiae* s.s (Lyimo *et al*., 1992) and that 28 °C was the optimal temperature for their rate of development (Bayoh and Lindsay, 2003). Since these optimal temperatures are approaching the average water temperatures in the field, it is suggested that the immature mosquitoes are evolutionarily adapted to their direct environment. It is likely that any differences in larval development and survival between the differently sized breeding sites

DOI: 10.1002/hyp

should be sought in the magnitude and duration of (a) the deviations from this mean or (b) the temperature change per unit time. The relationship between different daily fluctuations in water temperature and the life-history characteristics of mosquito immatures should be the subject of future studies.

Besides affecting the mosquito immatures directly, water temperature will have an effect on the diversity, densities and activity of other aquatic organisms, including possible predators, pathogens and food resources, such as algal matter, of the mosquito larvae. Moreover, water temperature affects hydrological parameters, such as dissolved oxygen, pH and conductivity (Losordo and Piedrahita, 1991).

Comparing these temperature data with temperature data of natural mosquito larval habitats described in other studies (Munga *et al*., 2005; Huang *et al*., 2006) remains difficult, since important parameters such as habitat dimensions (this study; Minakawa *et al*., 2004), water turbidity (Paaijmans *et al*., 2008) and factors affecting local microclimate such as land cover type and canopy overgrowth (Munga *et al*., 2006) and altitude will affect the water temperature. In the highlands of western Kenya, comparable maximum water temperatures are reached in farmland pools as in the studied small-sized water pool (Munga *et al*., 2005). The minimum and average water temperatures are, however, lower in the highlands. More detailed studies are required to show the effect of altitude on the local microclimate in such elevated areas in order to understand and predict water temperatures of mosquito larval habitats. These areas are affected by malaria (Malakooti *et al*., 1998) and higher altitudes within malaria areas will possible see an increase in malaria transmission due to the creation of a more suitable environment (Martens *et al*., 1995) under a changing global climate.

Remarkably, even within one single larval habitat large temperature differences may occur: average differences in water temperature of 2·9 (±2·6 standard deviation) and 3·1 (±2·4)°C have been recorded in dirt tracks and ditches, respectively, with a maximum difference within a single water pool (dirt track) of 9 °C (Koenraadt *et al*., 2004). This is possible in larger water pools, such as extended tyre-tracks on a dirt road or extended ditches, whereby some parts may be shaded and others sunlit, enlarging the difference.

The change in water temperature corresponded better to a change in incoming solar radiation at the small-sized water pool. This will be due to its small volume, which results in a small heat capacity. Larger water pools have a larger buffer capacity and, therefore, sudden changes in the local microclimate, such as a change in incoming solar radiation, will have less effect on the water temperature. The larger buffering capacity of the large-sized water pool was probably the reason that this water pool reached a lower minimum temperature on DOY 119 than on DOY 118. During the latter day the lowest value in the study period of the total incoming solar radiation load was recorded and all water pools were subjected to excessive rainfall, whereby the small-sized and medium-sized water pool reached a lower minimum temperature than on DOY 119.

During rainfall, decreases in water temperature were observed with a maximum decrease of 5 °C (in 15 min) in the small-sized water pool. The water level in this water pool was generally more susceptible to rainfall due to its smaller depth, which results in a higher precipitation-depth : water-depth ratio. Therefore a relatively large percentage of the water volume consists of the cooler rainwater during rainfall. However, the magnitude and direction of the change of the water temperature depends on parameters such as habitat dimensions, water temperature of the habitat, temperature of the rainwater, duration and quantity of the precipitation and the time of day when rainfall occurs.

Rainfall may also affect the daily average water temperature and the magnitude of the fluctuations around this mean. Bayoh (2001) observed a significant decrease in daily mean water temperature of both a puddle and a rice field after 6 days of rainfall. After the rains, mean hourly water temperatures decreased by up to 6 °C compared with water temperatures before the rains and the amplitude of the diurnal temperature was reduced. Young (1975) found similar results in Kenya: even in a large dammed pond (11 552 m^2) the daily mean water temperature dropped by almost 2–3 °C and diurnal fluctuations decreased by more than half after 1 day of rainfall.

Remarkably, the air temperature at 2 m above ground was below the water temperatures of all water pools throughout each day, even during the rapid increase of temperatures during the first hours after sunrise. Young (1975) observed that the average weekly air temperature was always below the average minimum weekly water temperature of the large dammed pond in Kenya mentioned above. Data from the present study showed that the organisms that live in small and shallow waters, such as larvae of *Anopheles gambiae* s.l., are exposed to temperatures that can differ considerably from the air temperature. The largest differences between air and water temperature during daytime were observed in the small-sized water pool, with a difference up to 10·2 °C, whereas the largest differences during night-time occurred in the large-sized water pool, with a difference up to 8·1 °C. The observed differences between air and water temperature have important consequences for ecological models that use the air temperature as an input parameter for larval development and survival (Hoshen and Morse, 2004). Air temperature can be used as an input parameter when the exact relationship between water temperature and air temperature is known. This study showed that there were strong and significant correlations between the average water temperature and various meteorological variables, including the average air temperature. This gives the opportunity to predict the average water temperature quite accurately using the average air temperature.

DOI: 10.1002/hyp

The exchange of heat across the air–water interface is considered one of the more important factors that govern the temperature of a water pool (Edinger *et al*., 1968). The air–water interface was the most important boundary for energy exchange with 83–88% of the energy being gained from shortwave and longwave radiation. Similar quantitative data have been reported by other studies (Webb and Zhang, 1997; Evans *et al*., 1998). The same interface was, furthermore, the most important boundary for energy losses; 82–89% of the losses occurred at this boundary, whereby longwave radiation (65–69%) accounted for the largest percentage of heat loss. The estimated average energy loss due to evaporation (15–18%) and the sensible heat exchange (<2·5%) was lower than the reported 24–30% and 5–11%, respectively, in other studies (Webb and Zhang, 1997; Evans *et al*., 1998). However, these studies were carried out in a different non-stagnant water system (a river) at a different geographical latitude, where climate is different and distinct seasons are present.

Although the contribution of the soil heat exchange to energy gains and losses is relatively small, both the exchange horizontally and sideways need to be incorporated in models that try to estimate water temperatures of very small water systems. These terms are not negligible due to the relatively small volume of the water pools compared with that of the rivers, ponds and lakes in other studies. It was believed that the thickness of the plastic foil did not interfere with the soil heat flux, as the heat conductivity of foil is approximately 0·15 W m^{-1} K^{-1} (Weast, 1984), which results in a heat resistance of the plastic foil used of $6{\cdot}7 \times 10^{-4}$ W^{-1} m^2 K. As this heat resistance is low, one may assume that the plastic foil will hardly affect the soil heat flux process.

When modelling small and shallow water pools, it is necessary to have accurate estimations of soil properties. Soil properties, such as heat conductivity, will depend largely on soil moisture, which will vary between days: in Kenya it can be extremely hot and dry one day and extremely wet the next. Therefore, by measuring the soil heat flux and soil moisture directly, our understanding of soil processes would improve. Hoshen and Morse (2004) suggested that the inclusion of hydrology and soil type may improve the understanding of the connection between precipitation and the larval habitats, but it may also provide useful information in order to estimate the diurnal water temperature behaviour of such habitats.

The use of the transfer coefficients for heat and water vapour, which were derived from measurement above a grassland surface and by using the typical values for the roughness length for heat and momentum above this type of surface cover, proved possible. As the grass was kept short, the areas with the meteorological stations were both open grasslands and the water pools were small, the microclimate above the water surfaces was similar to that above the surrounding grass surface. Changes in the surroundings, such as the presence of tall grass vegetation, or changes within a habitat, such as the presence of aquatic vegetation, may result in a reduction of wind (wind shielding) and radiation (a reduced view factor). This will require the introduction of correction-factors, as a standard weather station will not sense these changes in microclimate.

Evaporation is an important factor that determines the longevity of a water pool to a large extent. During clear days, small water pools will evaporate more during daytime than larger ones, as the difference between water temperature of smaller water pools and the surrounding air temperature are larger. In the evening the situation is reversed: the larger breeding sites will vaporize more water due to larger difference between their water temperature and the air temperature. When water pool dimensions decreased, more water vaporized cumulatively on clear and overcast days. On an extremely overcast day the situation was reversed.

The longevity of a breeding site depends on a range of other factors, such as soil structure, soil moisture, incoming water by precipitation and human disturbances, but this study illustrates the transient nature of natural mosquito breeding sites. The estimates imply that, with an average evaporation rate of 4·8 mm during clear days, the small-sized water pool would be desiccated within 8·3 days when no water is added. Therefore mosquito larvae that inhabit such small water pools only have a short time to develop into adults in the absence of rains, while it is known that larvae of *An. gambiae* s.l. may take between 1 and 3 weeks to develop into adult mosquitoes under ambient condition in the field (Jepson *et al*., 1947; Gimnig *et al*., 2002). However, desiccation of a habitat does not directly result in mortality of the immatures, since eggs of *An. gambiae* s.l. can remain viable for 12 days (Beier *et al*., 1990) and larvae are capable of surviving on moist mud from 64 h for the youngest larvae up to an estimated 113 h for the oldest larvae (Koenraadt *et al*., 2003).

The diurnal temperature dynamics of typical *An. gambiae* breeding sites were detailed and the importance of the various energy fluxes that contribute to the energy balance of such water pools assessed, including the amount of heat that is stored in the water volume, which eventually determines the diurnal water temperature behaviour. Besides being capable of predicting the water temperature now, it may be possible to estimate the magnitude of the changes in water temperatures under a changing global climate. Furthermore, these findings may be translated to other continents where similar or other mosquito species are transmitters of important vector-borne diseases.

ACKNOWLEDGEMENTS

Willy Hillen is thanked for constructing the floating equipment taking the water temperature readings. We also thank Paul Omondi and Constantine Otieno for their assistance during the field experiments and two anonymous reviewers for their constructive suggestions, which helped to improve this manuscript. This study was supported by the Netherlands Foundation for the

DOI: 10.1002/hyp

Advancement of Tropical Research (NWO/WOTRO; W93-409) and has been published with permission of the director of the Kenya Medical Research Institute.

REFERENCES

Andrewartha HG, Birch LC. 1954. *The Distribution and Abundance of Animals*. University of Chicago Press: Chicago.

Arya SP. 2001. *Introduction to Micrometeorology*. Academic Press: London.

Atkinson D. 1994. Temperature and organism size: a biological law for ectotherms. *Advances in Ecological Research* **25**: 1–58.

Bayoh MN. 2001. *Studies on the development and survival of Anopheles gambiae sensu stricto at various temperatures and relative humidities*. PhD thesis, University of Durham, Durham.

Bayoh MN, Lindsay SW. 2003. Effect of temperature on the development of the aquatic stages of *Anopheles gambiae* sensu stricto (Diptera: Culicidae). *Bulletin of Entomological Research* **93**: 375–381.

Bayoh MN, Lindsay SW. 2004. Temperature-related duration of aquatic stages of the Afrotropical malaria vector mosquito *Anopheles gambiae* in the laboratory. *Medical and Veterinary Entomology* **18**: 174–179.

Beier JC, Copeland R, Oyaro C, Masinya A, Odago WO, Oduor S, Koech DK, Roberts CR. 1990. *Anopheles gambiae* complex egg-stage survival in dry soil from larval development sites in western Kenya. *Journal of the American Mosquito Control Association* **6**: 105–109.

Beljaars ACM, Holtslag AAM. 1991. Flux parameterization over land surfaces for atmospheric models. *Journal of Applied Meteorology* **30**: 327–341.

Breman JG. 2001. The ears of the hippopotamus: manifestations, determinants, and estimates of the malaria burden. *American Journal of Tropical Medicine and Hygiene* **64**: 1–11.

Budyko MI. 1956. *The Heat Balance of the Earth's Surface* (translated from Russian). United States Weather Bureau: Washington.

Campbell GS, Norman JM. 2000. *An Introduction to Environmental Biophysics*. Springer: New York.

De Bruin HAR. 1982. Temperature and energy balance of a water reservoir determined from standard weather data of a land station. *Journal of Hydrology* **59**: 261–274.

Depinay J-MO, Mbogo CM, Killeen G, Knols B, Beier J, Carlson J, Dushoff J, Billingsley P, Mwambi H, Githure J, Toure AM, McKenzie FE. 2004. A simulation model of African *Anopheles* ecology and population dynamics for the analysis of malaria transmission. *Malaria Journal* **3**: 29.

Edinger JE, Duttweiler DW, Geyer JC. 1968. The response of water temperature to meteorological conditions. *Water Resources Research* **4**: 1137–1143.

Evans EC, McGregor GR, Petts GE. 1998. River energy budgets with special reference to river bed processes. *Hydrological Processes* **12**: 575–595.

Fillinger U, Sonye G, Killeen G, Knols BGJ, Becker N. 2004. The practical importance of permanent and semipermanent habitats for controlling aquatic stages of *Anopheles gambiae sensu lato* mosquitoes: operational observations from a rural town in western Kenya. *Tropical Medicine and International Health* **9**: 1274–1289.

Fraedrich K, Behlau A, Kerath G, Weber G. 1977. A simple model for estimating the evaporation from a shallow water reservoir. *Tellus* **29**: 428–434.

Frempong E. 1983. Diel aspects of the thermal structure and energy budget of a small English lake. *Freshwater Biology* **13**: 89–102.

Fritschen LJ, Gay LW. 1979. *Environmental instrumentation*. Springer-Verlag: New York.

Gillies MT, Coetzee M. 1987. *A supplement to the anophelinae of Africa south of the Sahara (Afrotropical region).* Publication no. 55. The South African Institute for Medical Research: Johannesburg.

Gillies MT, DeMeillon B. 1968. *The anophelinae of Africa south of the Sahara (Ethiopian zoogeographical region).* Publication no. 54. The South African Institute for Medical Research: Johannesburg.

Gimnig JE, Ombok M, Kamau L, Hawley WA. 2001. Characteristics of larval anopheline (Diptera: Culicidae) habitats in western Kenya. *Journal of Medical Entomology* **38**: 282–288.

Gimnig JE, Ombok M, Otieno S, Kaufman MG, Vulule JM, Walker ED. 2002. Density-dependent development of *Anopheles gambiae* (Diptera: Culicidae) larvae in artificial habitats. *Journal of Medical Entomology* **39**: 162–172.

Haddow AJ. 1943. Measurements of temperature and light in artificial pools with reference to the larval habitat of *Anopheles* (*Myzomyia*) *gambiae*, Giles, and *A. (M.) funestus*, Giles. *Bulletin of Entomological Research* **34**: 89–93.

Hagstrum DW, Workman EB. 1971. Interaction of temperature and feeding rate in determining the rate of development of larval *Culex tarsalis* (Diptera, Culicidae). *Annals of the Entomological Society of America* **64**: 668–671.

Hoshen MB, Morse AP. 2004. A weather-driven model of malaria transmission. *Malaria Journal* **3**: 32.

Huang J, Walker ED, Vulule J, Miller JR. 2006. Daily temperature profiles in and around Western Kenyan larval habitats of *Anopheles gambiae* as related to egg mortality. *Malaria Journal* **5**: 87.

Huffaker CB. 1944. The temperature relations of the immature stages of the malarial mosquito, *Anopheles quadrimaculatus* Say, with a comparison of the developmental power of constant and variable temperatures in insect metabolism. *Annals of the Entomological Society of America* **37**: 1–27.

Jacobs AFG, Jetten TH, Lucassen DC, Heusinkveld BG, Nieveen JP. 1997. Diurnal temperature fluctuations in a natural shallow water body. *Agricultural and Forest Meteorology* **88**: 269–277.

Jepson WF, Moutia A, Courtois C. 1947. The malaria problem in Mauritius: the bionomics of Mauritian anophelines. *Bulletin of Entomological Research* **38**: 177–208.

Keijman JQ. 1974. The estimation of the energy balance of a lake from simple weather data. *Boundary-Layer Meteorology* **7**: 399–407.

Koenraadt CJM, Paaijmans KP, Githeko AK, Knols BGJ, Takken W. 2003. Egg hatching, larval movement and larval survival of the malaria vector *Anopheles gambiae* in desiccating habitats. *Malaria Journal* **2**: 20.

Koenraadt CJM, Githeko AK, Takken W. 2004. The effects of rainfall and evapotranspiration on the temporal dynamics of *Anopheles gambiae* s.s. and *Anopheles arabiensis* in a Kenyan village. *Acta Tropica* **90**: 141–153.

Losordo TM, Piedrahita RH. 1991. Modelling temperature variation and thermal stratification in shallow aquaculture ponds. *Ecological Modelling* **54**: 189–226.

Lyimo EO, Takken W, Koella JC. 1992. Effect of rearing temperature and larval density on larval survival, age at pupation and adult size of *Anopheles gambiae*. *Entomologia Experimentalis et Applicata* **63**: 265–271.

Malakooti MA, Biomndo K, Shanks GD. 1998. Reemergence of epidemic malaria in the highlands of western Kenya. *Emerging Infectious Diseases* **4**: 671–676.

Martens WJM, Jetten TH, Rotmans J, Niessen LW. 1995. Climate change and vector-borne diseases—a global modelling perspective. *Global Environmental Change* **5**: 195–209.

Meier W, Bonjour C, Wüest A, Reichert P. 2003. Modeling the effect of water diversion on the temperature of mountain streams. *Journal of Environmental Engineering* **129**: 755–764.

Minakawa N, Sonye G, Mogi M, Yan G. 2004. Habitat characteristics of *Anopheles gambiae* s.s. larvae in a Kenyan highland. *Medical and Veterinary Entomology* **18**: 301–305.

Monteith JL, Unsworth MH. 1990. *Principles of Environmental Physics*. Edward Arnold: London.

Muchena FN. 1976. The soil resources of Maseno division, Kisumu district: a preliminary investigation. Kenya soil survey project, site evaluation report no. 27. Ministry of Agriculture, National Agricultural Laboratories, Nairobi.

Munga S, Minakawa N, Zhou G, Barrack O-OJ, Githeko AK, Yan G. 2005. Oviposition site preference and egg hatchability of *Anopheles gambiae*: effects of land cover types. *Journal of Medical Entomology* **42**: 993–997.

Munga S, Minakawa N, Zhou G, Mushinzimana E, Barrack O-OJ, Githeko AK, Yan G. 2006. Association between land cover and habitat productivity of malaria vectors in western Kenyan highlands. *American Journal of Tropical Medicine and Hygiene* **74**: 69–75.

Mutuku FM, Alaii JA, Bayoh MN, Gimnig JE, Vulule JM, Walker ED, Kabiru E, Hawley WA. 2006. Distribution, description, and local knowledge of larval habitats of *Anopheles gambiae* s.l. in a village in western Kenya. *American Journal of Tropical Medicine and Hygiene* **74**: 44–53.

Paaijmans KP, Takken W, Githeko AK, Jacobs AFG. 2008. The effect of water turbidity on the near-surface water temperature of larval habitats of the malaria mosquito *Anopheles gambiae*. *International Journal of Biometeorology* (in press). DOI: 10.1007/s00484-008-0167-2.

Shelton RM. 1973. The effect of temperatures on development of eight mosquito species. *Mosquito News* **33**: 1–12.

Sutherst RW, Maywald GF, Skarrat DB. 1995. Predicting insect distributions in a changed climate. In *Insects in a changing*

environment, Harrington R, Stork NE (eds). Academic Press: London; 59–91.

Tun-Lin W, Burkot TR, Kay BH. 2000. Effects of temperature and larval diet on development rates and survival of the dengue vector *Aedes aegypti* in north Queensland, Australia. *Medical and Veterinary Entomology* **14**: 31–37.

Tuno N, Miki K, Minakawa N, Githeko A, Yan G, Takagi M. 2004. Diving ability of *Anopheles gambiae* (Diptera: Culicidae) larvae. *Journal of Medical Entomology* **41**: 810–812.

Weast R. 1984. *CRC Handbook of Chemistry and Physics. A Ready-reference Book of Chemical and Physical Data*. Chemical Rubber Comp. Press: Cleveland, OH.

Webb BW, Zhang Y. 1997. Spatial and seasonal variability in the components of the river heat budget. *Hydrological Processes* **11**: 79–101.

WHO. 2005. *World Malaria Report 2005*. World Health Organization: Geneva.

Young JO. 1975. Seasonal and diurnal changes in the water temperature of a temperate pond (England) and a tropical pond (Kenya). *Hydrobiologia* **47**: 513–526.

Zhu S, Wang S, Deltour J. 2000. Modeling thermal stratification in aquaculture ponds. *Asian Fisheries Science* **13**: 169–182.

DOI: 10.1002/hyp